creasing the electron density on the phosphorus thus increasing the strength of the phosphorus–boron bond. It appears that (p → d)π bonding may also occur with second-row elements but to a much lesser extent. Structural studies seem to support the conclusion that the extent of (p → d)π bonding is greater between first- and second-row elements than between two second-row elements. For example, although nitrogen has a planar environment in H_2NPF_2,[15] the H_2PP moiety in H_2PPF_2 is not planar.[16] It has also been shown that while the heavy atoms in $(SiH_3)_3N$ are planar, those in $(SiH_3)_3P$ are not.[17] Results of other structural studies have been reviewed.[18] In a previous article we suggested that (p → d)π bonding played a part in determining the PF bond distance and the FPF bond angle in difluorophosphines.[3] If this argument is used, the Me_2NPF_2 and $MeOPF_2$, which display the longest PF bond distance and the smallest FPF bond angle, would be expected to be the best Lewis bases toward BH_3 in the series we examined. The unexpected strength of $MePF_2$ may be a result of some unexpected structural deformation which occurs when the borane adduct is formed. We are currently examining the structures of $MePF_2$ and $MePF_2 \cdot BH_3$ to determine if this is the case.

Although the position of $MePF_2$ as the strongest base in the series investigated cannot be explained by (p → d)π bonding since this type of bonding would be negligible for carbon, the electron-donating properties through σ donation of the methyl group and its subsequent effect upon the electron density of the phosphorus may be responsible for the high base strength of $MePF_2$. Another possible explanation might involve hyperconjugation between the C–H σ-bonding electrons and the phosphorus 3d orbitals. A combination of both σ-electron donation and hyperconjugation may be responsible for the observed basicity of $MePF_2$.

Although Coyle and Stone[19] suggested that B–H ir stretching frequencies can often be correlated to the strength of the boron–ligand bond in boron complexes, in our study the B–H stretching frequencies in the complexes investigated exhibit no simple relationships to the observed base strengths.

Acknowledgment.—The authors are grateful to the National Science Foundation for financial support. The authors are also grateful to Eric Roach of this department and Frank Parker of the University of Michigan for help in obtaining the ^{31}P and ^{11}B nmr spectra.

(15) A. H. Brittain, J. E. Smith, P. L. Lee, K. Cohn, and R. H. Schwendeman, *J. Amer. Chem. Soc.*, **93**, 6772 (1971).
(16) R. L. Kuczkowski, H. W. Schiller, and R. W. Rudolph, *Inorg. Chem.*, **10**, 2505 (1971).
(17) Z. B. Beagley, A. G. Robiette, and G. M. Sheldrick, *J. Chem. Soc. A*, 3002, 3006 (1968).
(18) L. D. Pettit, *Quart. Rev., Chem. Soc.*, **25**, 1 (1971).
(19) T. P. Coyle and F. G. A. Stone, "Progress in Boron Chemistry," Vol. 1, H. Steingerg and A. L. McCloskey, Ed., Macmillan, New York, N. Y., 1964.

CONTRIBUTION FROM THE DEPARTMENT OF CHEMISTRY AND THE MATERIALS RESEARCH CENTER, NORTHWESTERN UNIVERSITY, EVANSTON, ILLINOIS 60201

Molecular Beam Mass Spectra and Pyrolyses of Fluorophosphine–Triborane(7) Complexes. Formation and Mass Spectrum of Triborane(7)[1,2]

BY ROBERT T. PAINE, GOTTFRIED SODECK, AND FRED E. STAFFORD*

Received December 3, 1971

A molecular beam mass spectrometric characterization of $(CH_3)_2NF_2P \cdot {}^nB_3H_7$, $(CH_3)_2NF_2P \cdot {}^{10}B_3H_7$, and $F_3P \cdot {}^nB_3H_7$ and their respective pyrolysis products has been accomplished. The thermal decomposition of $(CH_3)_2NF_2P \cdot B_3H_7$ provided the first high-yield synthesis of the previously unobserved B_3H_7 reactive intermediate. The triborane(7) was characterized by mass spectrometric techniques, and its polyisotopic and ^{10}B enriched mass spectra are presented. The low parent ion intensity, $I(B_3H_7^+)$, suggests that the neutral progenitor B_3H_7 should be classified as an "unstable" borane. Decomposition of $(CH_3)_2NF_2P \cdot B_3H_7$ at room temperature also resulted in formation of $(CH_3)_2NF_2P \cdot B_4H_8$ which in turn acted as a high-yield source of B_4H_8. At elevated temperatures B_5H_x and B_6H_x species are formed. The appearance potentials of the principal ions are reported. The $F_3P \cdot B_3H_7$ complex decomposed at room temperature; however, the decomposition did not provide a good synthesis of B_3H_7. Attempts to prepare B_3H_9 were unsuccessful.

Introduction

The systematic formation of higher boranes, B_4H_{10}, B_5H_{11}, ..., during the pyrolysis of B_2H_6 has been long recognized[3] and actively investigated.[4-6] The initial steps of a commonly accepted mechanism[4-6] are

$$B_2H_6 \rightleftharpoons 2BH_3 \quad (1)$$

$$BH_3 + B_2H_6 \rightleftharpoons B_3H_9 \quad (2)$$

$$B_3H_9 \rightleftharpoons B_3H_7 + H_2 \quad (3)$$

$$B_3H_7 + B_2H_6 \rightleftharpoons B_4H_{10} + BH_3 \quad (4)$$

$$B_4H_{10} \longrightarrow B_4H_8 + H_2 \quad (5)$$

$$B_4H_8 + B_2H_6 \longrightarrow B_5H_{11} + BH_3 \quad (6)$$

Another step has been proposed

$$B_4H_{10} \longrightarrow B_3H_7 + BH_3 \quad (7)$$

(1) This work was supported by the U. S. Atomic Energy Commission, Document COO-1147-38.
(2) Presented in part at the 162nd National Meeting of the American Chemical Society, Washington, D. C., Sept 1971; see Abstracts, No. INOR 2.
(3) A. E. Stock, "Hydrides of Boron and Silicon," Cornell University Press, Ithaca, New York, 1933.
(4) The kinetic and mechanistic investigations of boron hydride pyrolysis reactions have been summarized in several review articles: (a) R. L. Hughes, I. C. Smith, and E. W. Lawless, "Production of the Boranes and Related Research," R. T. Holzmann, Ed., Academic Press, New York, N. Y., 1967; (b) R. W. Parry and M. K. Walter, "Preparative Inorganic Reactions," W. L. Jolly, Ed., Interscience Publishers, New York, N. Y., 1968; (c) W. N. Lipscomb, "Boron Hydrides," W. A. Benjamin, New York, N. Y., 1963; (d) R. M. Adams, "Boron, Metallo-Boron Compounds and Boranes," R. M. Adams, Ed., Interscience Publishers, New York, N. Y., 1964.
(5) R. Schaeffer, *J. Inorg. Nucl. Chem.*, **15**, 190 (1960).
(6) R. E. Enrione and R. Schaeffer, *ibid.*, **18**, 103 (1961).

As outlined, this mechanism and others[4,7] depend upon the existence of several reactive intermediates, *e.g.*, BH_3, B_3H_7, B_3H_9, B_4H_8. Consequently, the identification of these proposed species has been of interest.

In previous investigations two intermediates, BH_3 and B_4H_8, had been synthesized in high yields under specific conditions[8-10] and characterized by mass spectrometry[8-12] and matrix isolation infrared spectroscopy.[13] The particularly important triborane intermediates, B_3H_7 and B_3H_9, however, had not been identified conclusively.

Several synthetic routes to B_3H_7 are possible: pyrolysis of B_2H_6 (eq 1-3), the dissociation of B_4H_{10} (eq 7), the reaction of BH_3 and B_2H_6 (eq 2,3), and the dissociation of a weak base–triborane(7) complex. To date, attempts to identify B_3H_7 in the products from the pyrolyses of B_2H_6[11] or B_4H_{10}[12] have been unsuccessful. Furthermore, a triborane species obtained by Fridmann and Fehlner[14] from the gas-phase reaction of BH_3 with B_2H_6 has not been identified as B_3H_7 or B_3H_9.

The successful high-yield syntheses of BH_3 and B_4H_8 from the thermal decomposition of unstable Lewis acid–base complexes, *e.g.*, $OC \cdot BH_3$,[8,9] $F_3P \cdot BH_3$,[14] and $OC \cdot B_4H_8$,[10] suggested a similar application for the triborane(7) system. This paper reports the molecular beam mass spectrometric characterization of the relatively unstable $F_3P \cdot B_3H_7$[15] and stable $(CH_3)_2NF_2P \cdot B_3H_7$[16,17] complexes. The flow reactor pyrolysis of these complexes and the high-yield synthesis and mass spectral characterization of B_3H_7 are described. An attempted synthesis of B_3H_9 is outlined.

Experimental Section

Synthesis of Starting Materials.—Standard high-vacuum techniques were used for the manipulation of the volatile compounds.[18] Tetraborane(10) was prepared by the reaction of $[(CH_3)_4N][B_3H_8]$ with polyphosphoric acid[19] and by the "hot–cold" tube pyrolysis of $^nB_2H_6$.[20] A sample of $^{10}B_4H_{10}$ (96% ^{10}B and 4% ^{11}B[21]) was available from the past work of Hollins.[10] Trifluorophosphine was purchased from Ozark-Mahoning Co., Tulsa, Okla., and was purified by repeated trap to trap fractionation. The $(CH_3)_2NPF_2$ ligand was prepared as described by Fleming.[16]

The samples of $(CH_3)_2NF_2P \cdot {}^nB_3H_7$ were prepared as described by Fleming[16] and by Lory and Ritter[17] from the reaction of $^nB_4H_{10}$ and $(CH_3)_2NPF_2$. The volatile products were vacuum distilled through traps cooled to −24, −78, and −196°. The triborane(7) complex retained at −24° was purified by repeated distillation from 0 to −24°. The sample of $(CH_3)_2NF_2P \cdot {}^{10}B_3H_7$ was prepared in the same fashion. The $F_3P \cdot {}^nB_3H_7$ samples were prepared and purified as described by Paine and Parry.[15] The purity of the samples before and after examination with the mass spectrometer was verified by melting point and ^{19}F nmr spectroscopy. The samples were stored in glass break-seal tubes at −196°.

Mass Spectrometer.—The mass spectrometer used in this study was the 60°, 12 in. sector instrument described in previous publications from this laboratory.[11,22,23] A sample tube was joined to the gas inlet system by a glass–metal seal. The complexes were distilled through the broken, glass break-seal, copper and stainless steel tubing (*ca.* 8 in. long, 1/4-in. i.d.), a Nupro valve, and a Hoke valve[24] (both fully open) into the baffled, stainless steel Knudsen cell (reactor orifice 1.01 mm diameter, contact time $\sim 10^{1.5}$ msec). A constant, low-pressure flow was maintained by keeping $(CH_3)_2NF_2P \cdot B_3H_7$ at −45° and $F_3P \cdot B_3H_7$ at −126°. Reproducible reactor pressures ($\sim 7 \times 10^{-3}$ Torr) were easily achieved. No radiation shields were used in this study.[25] The reactor temperature was maintained by radiation from a tungsten filament regulated with a Thermac (Research Inc., Minneapolis, Minn.) proportional controller. All ion intensity and appearance potential measurements were recorded with the heating filaments on.

The molecular beam effusing from the reactor was ionized by 70 eV electrons except during appearance potential determinations. The ions formed were accelerated through a 4 kV potential, then mass analyzed and detected by a 20 stage Cu–Be secondary electron multiplier with 3.2 kV across the dynodes. The ion current data and the instrument settings were automatically read into a DEC (Digital Equipment Corp., Maynard, Mass.) PDP-8S digital computer and processed.[26] The ion current readings with shutter centered and displaced were time averaged for 20 sec. Appearance potentials were measured by the vanishing current method using time averaged ionization efficiency curves.[26] Argon leaked into the spectrometer and HCl and H_2O present as instrument background gases were used as electron energy calibrants.

The observed ions and their neutral progenitors were identified by their mass to charge ratio, mass defect, isotope ratio, shutter profile,[27] shutter effect,[28] and ion intensity–temperature dependence. The molecular beam intensity of selected ions as a function of inlet valve setting (open–closed) was also determined.

Data and Results

A. $(CH_3)_2NF_2P \cdot {}^nB_3H_7$. Molecular Beam Mass Spectrum.[29]—When the vapors above the solid $(CH_3)_2NF_2P \cdot {}^nB_3H_7$ (−45°) were passed through the reactor (25°) the molecular beam (mb) mass spectrum shown in Figure 1 was obtained. The spectrum was searched to m/e 350, but no ions above m/e 165 were observed (detectability limit of 0.2%). The principal ion envelopes observed, m/e 165–159, 153–146, 127–125,

(7) L. H. Long, *J. Inorg. Nucl. Chem.*, **32**, 1097 (1970).
(8) G. W. Mappes and T. P. Fehlner, *J. Amer. Chem. Soc.*, **92**, 1562 (1970).
(9) O. Herstad, G. A. Pressley, Jr., and F. E. Stafford, *J. Phys. Chem.*, **74**, 874 (1970).
(10) R. E. Hollins and F. E. Stafford, *Inorg. Chem.*, **9**, 877 (1970).
(11) A. B. Baylis, G. A. Pressley, Jr., and F. E. Stafford, *J. Amer. Chem. Soc.*, **88**, 2428 (1966).
(12) A. B. Baylis, G. A. Pressley, Jr., M. E. Gordon, and F. E. Stafford, *ibid.*, **88**, 929 (1966).
(13) A. Kaldor and R. Porter, *ibid.*, **93**, 2140 (1971).
(14) S. A. Fridmann and T. P. Fehlner, *ibid.*, **93**, 2824 (1971).
(15) R. T. Paine and R. W. Parry, *Inorg. Chem.*, **11**, 268 (1972).
(16) M. A. Fleming, Ph.D. Thesis, University of Michigan, Ann Arbor, Mich., 1963.
(17) E. R. Lory and D. M. Ritter, *Inorg. Chem.*, **10**, 939 (1971).
(18) D. F. Shriver, "The Manipulation of Air-Sensitive Compounds," McGraw-Hill, New York, N. Y., 1969.
(19) D. F. Gaines and R. Schaeffer, *Inorg. Chem.*, **3**, 438 (1964).
(20) M. J. Klein, B. C. Harrison, and I. J. Solomon, *J. Amer. Chem. Soc.*, **80**, 4149 (1958).
(21) Analysis given by the supplier, U. S. Atomic Energy Commission, Oak Ridge, Tenn., specifies a minimum of 96% ^{10}B in $CaF_2 \cdot {}^{10}BF_3$.
(22) F. E. Stafford, G. A. Pressley, Jr., and A. B. Baylis, *Advan. Chem. Ser.*, **No. 72**, 139 (1967).
(23) The mass spectrometer was built by Nuclide Associates, State College, Pa., Model 12-60-HT.
(24) Nupro valve B-4H, Nuclear Products Co., Cleveland, Ohio; Hoke Inc., Catalog No. 417A, Cresskil, N. J.
(25) The radiation shields were omitted since relatively low reactor temperatures (<300°) were employed. This had several important benefits: (1) reactor temperature equilibration time was reduced; (2) hot surfaces where decomposition of reactive species might occur were eliminated; and (3) pumping speed in the flow reactor region was increased.
(26) J. R. Wyatt, G. A. Pressley, Jr., and F. E. Stafford, *High Temp. Sci.*, **3**, 130 (1970).
(27) A plot of ion intensity *vs.* shutter position produces a shutter profile. The shape of the profile indicates whether the observed species originate from the crucible orifice, crucible lid, heating elements, etc. Molecules identified as originating directly from the orifice pass through the ion source without pyrolysis on the hot ion source surfaces, hence the importance of the molecular beam mass spectra.
(28) The ratio of ion intensity due to species diffusing directly from the orifice (molecular beam species) to the total ion intensity at a given mass peak is called the "per cent shutter effect." Highly reactive species, which are expected to be destroyed by every collision with the spectrometer walls, have high shutter effects (~100%), while stable species have small shutter effects (*e.g.*, 5–10% for Ar and 15–25% for nonreactive boranes, B_2H_6,[11] B_4H_{10},[12] B_5H_9,[10] B_5H_{11}[10]).
(29) The molecular beam mass spectrum is defined as that recorded at the lowest possible reactor temperature (25°). This differs from a "conventional" spectrum which is obtained with an ion source thermostated at, *e.g.*, 125°. The conventional source can act as a flow reactor to produce a mixture of sample molecules, reactive intermediates, and pyrolysis products.

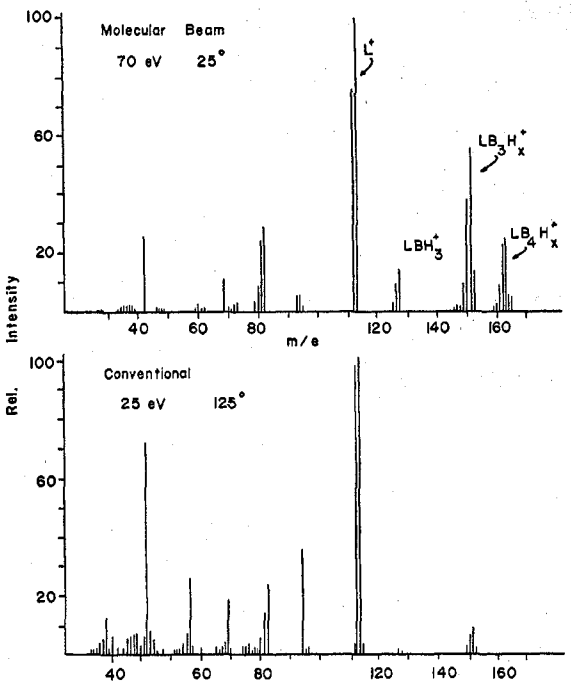

Figure 1.—$(CH_3)_2NF_2P \cdot {}^nB_3H_7$ mass spectra. Top: molecular beam mass spectrum (ionizing voltage 70 eV, reactor temperature 25°). Bottom: conventional mass spectrum[17] (ionizing voltage 25 eV, ion source temperature 125°). The peaks in the top spectrum at *m/e* 159–165 are due to $(CH_3)_2NF_2P \cdot B_4H_x^+$. The reduced parent and increased fragment ion intensities in the lower spectrum are ascribed to pyrolysis of the complex in the ion source.

113–112, were assigned to $(CH_3)_2NF_2P \cdot B_4H_x^+$, $(CH_3)_2NF_2P \cdot B_3H_x^+$, $(CH_3)_2NF_2P \cdot BH_x^+$, and $(CH_x)_2NF_2P^+$, respectively. The neutral progenitors of these ions and of the lower mass fragments were identified as $(CH_3)_2NF_2P \cdot B_4H_8$ and $(CH_3)_2NF_2P \cdot B_3H_7$. Contributions to the mb $L \cdot B_3H_x^+$ intensities from electron impact fragmentation of $L \cdot B_4H_8$ at 25° were estimated to be small.[30] Shutter profiles for $L \cdot B_4H_x^+$ and $L \cdot B_3H_x^+$ ions indicate that their neutral progenitors effuse from the reactor and not from metal surfaces surrounding the reactor or ion source.

The appearance potentials of the principal ions at 25° are listed in Table I. The AP for $L \cdot B_3H_7^+$ could not be measured due to the low ion intensity. If the neutral progenitor of the $L \cdot B_3H_x^+$ ions was $L \cdot B_4H_8$ then the appearance potentials of the $L \cdot B_3H_x^+$ ions should have been greater than those observed.

The "conventional" mass spectrum recorded on an AEI MS-9 spectrometer (ionizing voltage 25 eV, source temperature ~125°)[17,31] is compared with the mb mass spectrum in Figure 1. Some important differences are readily apparent. The mb spectrum shows the following: (1) an envelope of peaks corresponding to $L \cdot B_4H_x^+$ (*m/e* 159–165) not observed in the conventional spectrum, (2) a more intense parent ion envelope corresponding to $L \cdot B_3H_x^+$ (*m/e* 146–152), and (3) decreased ion intensities in the region *m/e* 10–100 corresponding to lower mb intensities for $B_4H_x^+$, $B_6H_x^+$, $B_6H_x^+$, and ligand fragment ions (see Discussion).

(30) An estimate of the contribution to $LB_3H_x^+$ ion intensities from $L \cdot B_4H_8$ neutral can be made from the work of Hollins,[10] *e.g.*, $\Sigma I(OC \cdot B_4H_x^+)/\Sigma I(OC \cdot B_3H_x^+) > 4$. This suggests that only ~1/8 of $\Sigma I[(CH_3)_2NF_2P \cdot B_3H_x^+]$ may result from fragmentation of $L \cdot B_4H_8$.

(31) Private communication from E. R. Lory.

TABLE I

APPEARANCE POTENTIALS FOR $(CH_3)_2NF_2P \cdot {}^nB_3H_7$

Neutral progenitor		*m/e*	AP, eV[a]
	A. Reactor at 25°		
$L \cdot B_4H_8 + e^-$	→	165 p[b]	9.6
		164 p_i	9.8
		163	10.0
$L \cdot B_3H_7 + e^-$	→	152 p–H	10.5
		151	10.4
$L \cdot BH_3(?) + e^-$	→	127	12.2
$L + e^-$	→	113 p	10.2
	B. Reactor at 125°		
$B_4H_8 + e^-$	→	48	10.9
$B_3H_7 + e^-$	→	39 p–H	11.2
		38	11.5

[a] The estimated uncertainty in AP measurements for each ion is ±0.3 eV and represents the reproducibility. [b] p = parent; $p_i = {}^{11}B_3{}^{10}BH_8^+$.

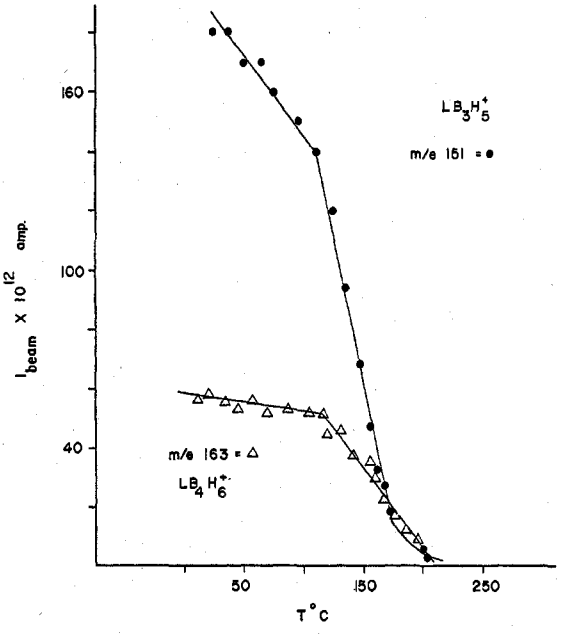

Figure 2.—Thermal decomposition of $(CH_3)_2NF_2P \cdot {}^nB_3H_7$ and $(CH_3)_2NF_2P \cdot {}^nB_4H_8$; absolute intensities for *m/e* 151 (●) and 163 (△) as functions of reactor temperature.

Several observations indicate that $L \cdot B_4H_8$ was not present as an impurity in the original cold (−45°) $L \cdot B_3H_7$ vapors which were distilled into the inlet system of the spectrometer. The ratio of observed ion intensities $\Sigma I(L \cdot B_3H_x^+)/(\Sigma I(L \cdot B_4H_x^+) = 2.3 \pm 0.2$ was constant with three different samples (prepared independently of each other) and remained constant during all investigations (from initial opening of the sample until the sample was exhausted). The melting point of each sample (−35.1 ± 0.5°) was in good agreement with the known value[17] for $(CH_3)_2NF_2P \cdot B_3H_7$ (−35.5). The ^{19}F nmr spectra of two samples recorded before and after mass spectral examination showed no impurity peaks. The presence of 10% $L \cdot B_4H_8$ in $L \cdot B_3H_7$ should have been detected by our nmr experiments. In addition, $(CH_3)_2NF_2P \cdot B_4H_8$ has not been detected in $(CH_3)_2NF_2P \cdot B_3H_7$ samples when the latter have been subjected to gas chromatographic analysis.[31]

Thermal Decomposition.—The mb intensity varia-

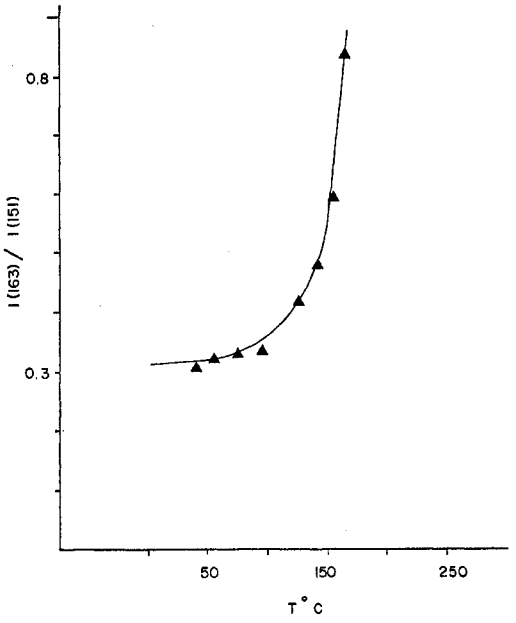

Figure 3.—Decomposition of $(CH_3)_2NF_2P \cdot B_3H_7$; intensity of m/e 163 relative to intensity of m/e 151 as a function of temperature. The sharp increase in the ratio is due to pyrolysis of $L \cdot B_3H_7$ before $L \cdot B_4H_8$.

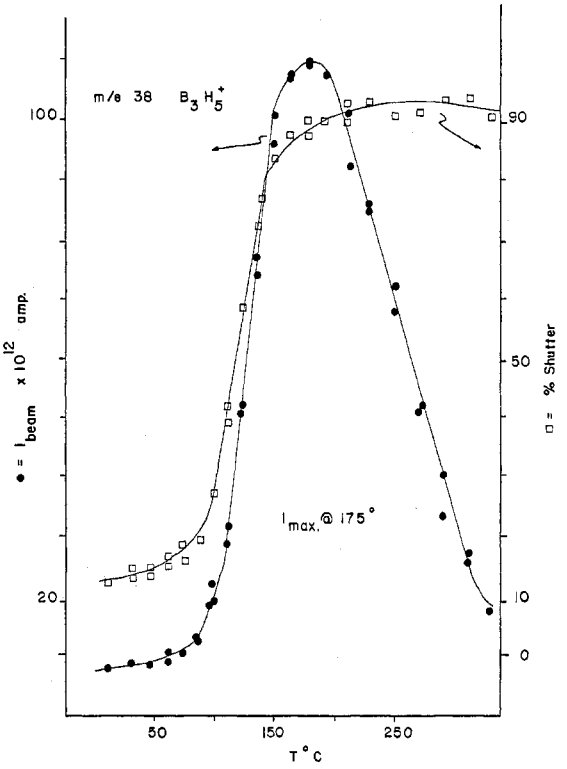

Figure 4.—Formation and disappearance of triborane (7); absolute intensity (●), amps, and shutter effect (□) for m/e 38 ($B_3H_5^+$) as functions of temperature. The sharp rise in per cent shutter effect is diagnostic of the formation of a reactive species.

tions with temperature for m/e 151 and 163 are shown in Figure 2. The average temperatures (four determinations) at which the complexes were *ca.* 95% decomposed were 185 ± 10° and 205 ± 10°,[32] respec-

(32) The indicated uncertainty in temperature refers to the reproducibility of measuring the pyrolysis maxima over four determinations and not to any error in actual thermocouple readings.

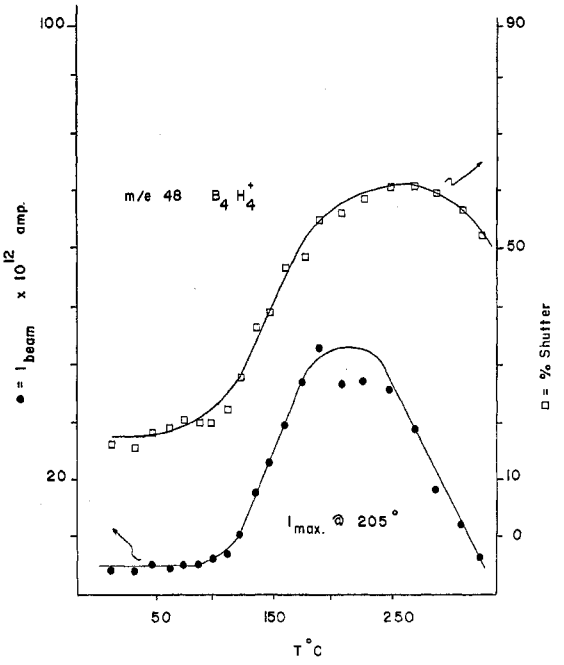

Figure 5.—Formation and disappearance of tetraborane(8); absolute intensity (●), amps, and shutter effect (□) for m/e 48 ($B_4H_4^+$) as functions of temperature.

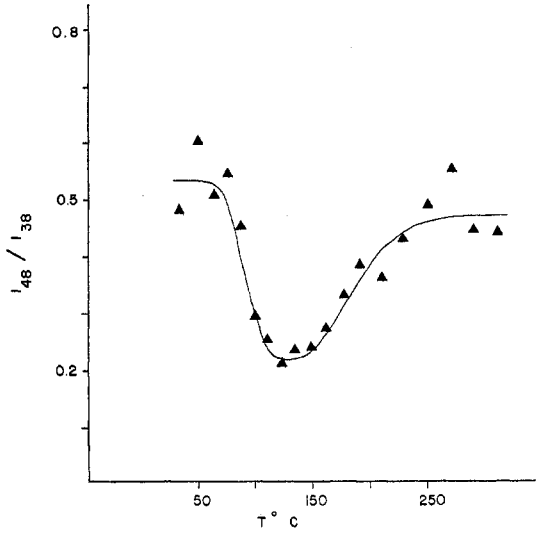

Figure 6.—Variation of $I(48)/I(38)$ $[I(B_4H_4^+)/I(B_3H_5^+)]$ *vs.* temperature.

tively. The small decrease of ion intensity for m/e 163 relative to m/e 151 in the temperature range 25–110° suggests that $L \cdot B_4H_8$ is more thermally stable than $L \cdot B_3H_7$.

The variation of the ratio $I(163)/I(151)$ with temperature is shown in Figure 3. All fragment ions with the same neutral progenitor should have the same I^+ *vs.* T dependence. The nonlinear temperature dependence clearly indicates that $L \cdot B_3H_x^+$ ions were not electron impact fragments of $L \cdot B_4H_8$. The observed sharp increase in the ion ratio is consistent with decomposition of $L \cdot B_3H_7$ before $L \cdot B_4H_8$.

Concurrent with the rapid decrease in absolute mb intensity for $L \cdot B_4H_x^+$ and $L \cdot B_3H_x^+$ ions were rapid increases in absolute mb intensities and per cent shutter effects for the $B_3H_x^+$ and $B_4H_x^+$ ions. The variations

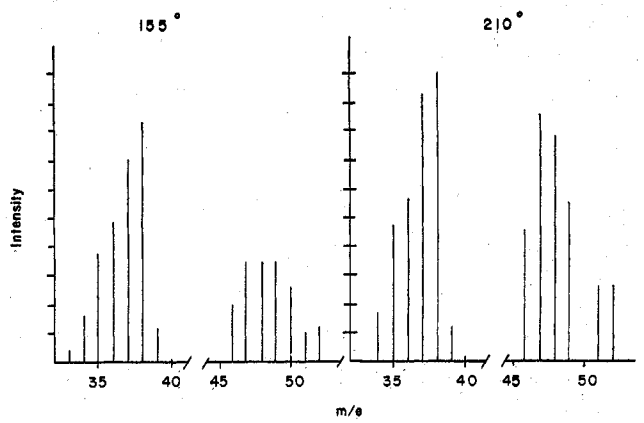

Figure 7. Polyisotopic borane ($^nB_yH_x$, y = 3 and 4) mass spectra (ionizing voltage 70 eV) with reactor temperatures of 155 and 210°.

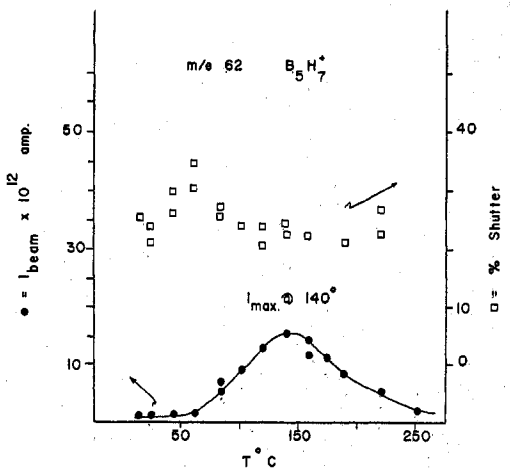

Figure 8. Formation and disappearance of pentaborane(s); absolute intensity (●), amps, and shutter effect (□) for m/e 62 as functions of temperature.

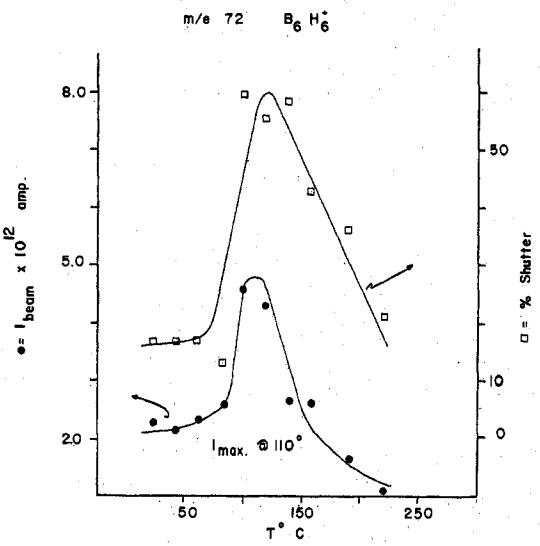

Figure 9. Formation and disappearance of hexaborane(s); absolute intensity (●), amps, and shutter effect (□) for m/e 72 as functions of temperature.

of $I(38)$ and $I(48)$ with temperature are shown in Figures 4 and 5. From room temperature to *ca.* 80° (m/e 38) and *ca.* 100° (m/e 48) the mb intensities and shutter effects were constant. Above 100° the

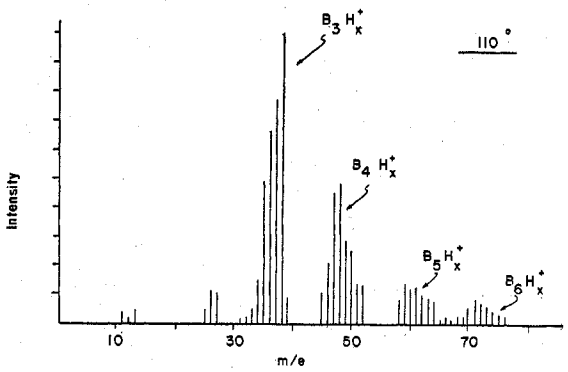

Figure 10. Polyisotopic borane ($^nB_yH_x^+$) mass spectrum of vapors effusing from reactor (ionizing voltage 70 eV, reactor temperature 110°).

ion intensities and shutter effects increased rapidly. The mb intensities maximized at 175 ± 15° (m/e 38) and at 205 ± 15° (m/e 48). The latter maximum agrees with previous B_4H_8 syntheses from $OC{\cdot}B_4H_8$ (175–210°)[10] and from B_5H_{11} (175–195°).[10] Further increase in the reactor temperature resulted in decreasing mb intensities. The respective shutter effects maximized at 95% (m/e 38) and 60% (m/e 48). The same behavior was observed for m/e 37 and 47. Shutter profiles of m/e 37, 38, 39, 48, 49 in the temperature range 150–200° confirm that the neutral progenitors originate solely from the reactor. These results are consistent with the formation of neutral reactive intermediates B_3H_7 and B_4H_8. Furthermore the nonlinear variation of the ion intensity ratio $I(48)/I(38)$ with temperature shown in Figure 6 indicates that B_4H_8 is not a significant source of triborane ions between 75 and 225°. Appearance potentials for the principal $B_3H_x^+$ and $B_4H_x^+$ ions at 125° are listed in Table I. If $B_3H_x^+$ ions originated from fragmentation of a higher boron hydride, *e.g.*, B_4H_8, then higher AP's should have been observed. The AP for the parent ionizaton process, $B_3H_7 + e^- \rightarrow B_3H_7^+ + \ldots$, could not be measured due to the low ion intensity.

The mass spectra of the triborane and tetraborane species recorded near their respective I_{max} temperatures are shown in Figure 7. The very small parent ion intensity (0.2) of triborane(7) (m/e 40) is noteworthy and will be discussed. The tetraborane region, m/e 52–46, is identical with the polyisotopic spectrum obtained by Hollins and Stafford.[10]

The formation of $B_3H_x^+$ and $B_4H_x^+$ ions was accompanied by the formation of higher boranes. Figures 8 and 9 describe the variation in mb intensities with temperature of $B_5H_7^+$ (m/e 62) and $B_6H_6^+$ (m/e 72). The mb intensity maxima are 140 ± 10° (m/e 62) and 110 ± 10° (m/e 72). The absolute intensities, $I(62)$ and $I(72)$ and the intensity sums, $\Sigma I(B_5H_x^+)$ and $\Sigma I(B_6H_x^+)$, indicate that the pentaborane(s) were about three times more abundant in the molecular beam than the hexaborane(s).

The mass spectrum m/e 10–80 (ligand peaks subtracted out) with the reactor at 110° is shown in Figure 10. The triborane ion intensities are listed in Table II. At this temperature B_3H_7, B_4H_8, pentaborane, and hexaborane pyrolysis products all were present in significant amounts. By comparison with known fragmentation patterns, the contributions to

TABLE II
OBSERVED MASS SPECTRA OF TRIBORANES

m/e	$^{n}B_3H_7$[a] (110°)	$^{10}B_3H_7$[a] (130°)
40	0.2 ± 0.2[b]	
39	11 ± 5	0.5 ± 0.5
38	100	0.5 ± 0.5
37	75 ± 8	1 ± 1
36	66 ± 9	16 ± 8
35	48 ± 10	100
34	18 ± 8	21 ± 9
33	5 ± 3	60 ± 9
32		16 ± 7
31		8 ± 4
30		

[a] From the pyrolysis of $(CH_3)_2NF_2P\cdot{}^{n}B_3H_7$ and $(CH_3)_2NF_2P\cdot{}^{10}B_3H_7$ (^{11}B enriched), see text. Contributions from B_4H_x and higher borane fragmentation have not been subtracted out; however, their contributions are known to be small. [b] Background intensity in the region *m/e* 42–40 was high; hence small ion intensities were measured with considerable uncertainty.

the $B_3H_x^+$ ion intensities from higher borane fragmentation are estimated to be small.

With the reactor at 25°, inlet-valve "open–closed" experiments indicate that $L\cdot B_4H_x^+$, $L\cdot B_3H_x^+$, $B_3H_x^+$, $B_4H_x^+$, $B_5H_x^+$, and $B_6H_x^+$ ion intensities decreased very slowly (~90% intensity decay in 2.0–2.5 min) upon closing the valve. At higher reactor temperatures (110–200°) all ion intensities decreased very rapidly (~90% intensity decay in 3 sec) upon closing the valve. The ion intensity due to the ligand parent ion, $(CH_3)_2NPF_2^+$ (*m/e* 113), however, decreased very rapidly at all temperatures, 25–200°. These results are consistent with sorption of the neutral species $L\cdot B_4H_8$, $L\cdot B_3H_7$, B_5H_x, and B_6H_x on the walls of the inlet system and reactor at 25°.

B. $(CH_3)_2NF_2P\cdot{}^{10}B_3H_7$. Molecular Beam Mass Spectrum.—An investigation of a ^{10}B isotopically enriched sample was undertaken. The lower background intensity in the region *m/e* 37–39 compared to *m/e* 40–42 was expected to allow more accurate measurement of the parent ion $B_3H_7^+$. The mb mass spectrum that was recorded was comparable to the normal isotopic spectrum and therefore will not be described. The ratio $\Sigma I(L\cdot B_3H_x^+)/\Sigma I(L\cdot B_4H_x^+) \cong 2.2$ was identical with that found for the normal isotopic samples.

Thermal Decomposition.—The pyrolysis behavior of $L\cdot{}^{10}B_3H_5^+$ (*m/e* 148) was identical with that shown in Figure 2 for $L\cdot{}^{n}B_3H_5^+$. The variation in mb intensity with temperature for $^{10}B_3H_5^+$ (*m/e* 35) was similar to that shown in Figure 4 for $^{n}B_3H_5^+$ (ion intensity maximum at 170 ± 10°). The triborane parent ion region was recorded at 130°. The intensities relative to *m/e* 35 are listed and compared with the normal isotope spectrum in Table II.

C. Attempted Synthesis of B_3H_9.—An attempt was made to synthesize B_3H_9 in the reactor by the reaction $B_3H_7 + H_2 \rightarrow B_3H_9$. A second gas inlet system was introduced between the $L\cdot B_3H_7$ sample tube and the reactor. Hydrogen gas was leaked into the stream of $L\cdot{}^{10}B_3H_7$, and the mixture flowed into the reactor. Hydrogen partial pressures up to 100 times that of the complex were used (total reactor pressure *ca.* 0.1 Torr). Small changes in the ion intensities at *m/e* 32–37 were noted in the temperature range 100–130°, but no significant intensity change occurred at *m/e* 38 or 39.

D. $F_3P\cdot{}^{n}B_3H_7$. Molecular Beam Mass Spectrum.—The reaction chemistry of $F_3P\cdot B_3H_7$[15] indicates that this complex is less stable than $(CH_3)_2NF_2P\cdot B_3H_7$ and therefore a good candidate for a high-yield synthesis of B_3H_7.

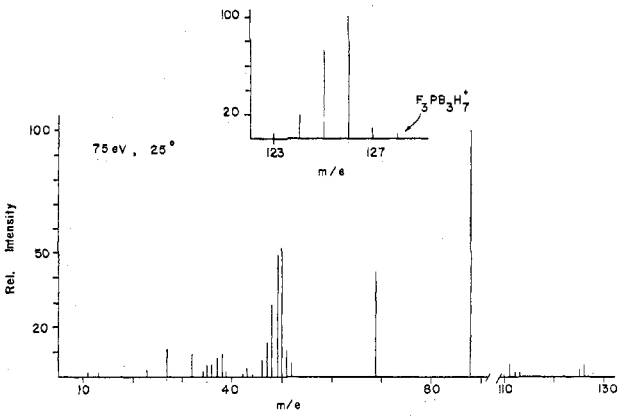

Figure 11. Mass spectrum of the vapors above $F_3P\cdot{}^{n}B_3H_7$ (ionizing voltage 70 eV, reactor temperature 25°) normalized to $I(F_3P^+)$ *m/e* 88. Inset spectrum is of the parent-ion region normalized to *m/e* 126.

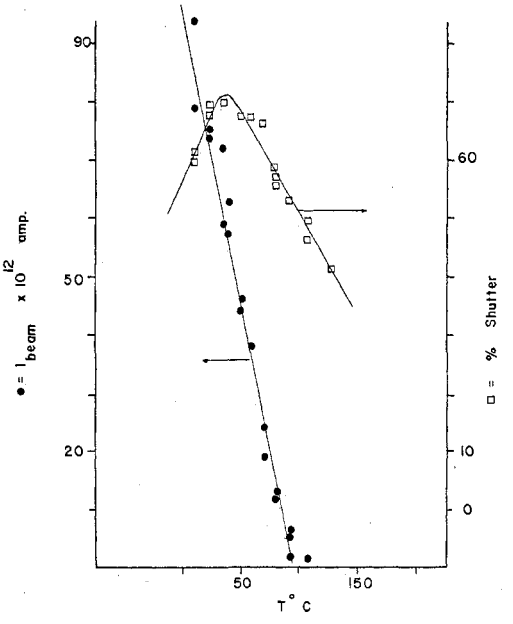

Figure 12. Thermal decomposition of $F_3P\cdot{}^{n}B_3H_7$; absolute intensity (●), amps, and shutter effect (□) for *m/e* 126 as functions of temperature.

The molecular beam mass spectrum of $F_3P\cdot{}^{n}B_3H_7$ is shown in Figure 11. The spectrum is similar to that obtained by conventional mass spectrometry.[15] The mb spectrum, *m/e* 10–130, is normalized to PF_3^+ (*m/e* 88), and the inset spectrum of the parent region, *m/e* 122–129, is normalized to *m/e* 126. The parent ion $F_3PB_3H_7^+$ (*m/e* 128) intensity is very small. The parent fragmentation envelope (*m/e* 128–121) is comparable in shape to the parent envelope of $(CH_3)_2NF_2P\cdot B_3H_7$ (Figure 1), but the remainder of the $F_3P\cdot B_3H_7$ mb spectrum is different from that of $(CH_3)_2NF_2P\cdot B_3H_7$. In particular, there is an intense $B_4H_x^+$ fragmentation envelope (*m/e* 52–47), which is comparable to the known fragmentation pattern of B_4H_{10}. At present, however, the neutral progenitor of the $B_4H_x^+$ ions has not been finally identified. The appearance potential for the ion $F_3P\cdot B_3H_5^+$ was 10.8 ± 0.3 eV (25°).

Thermal Decomposition.—The temperature depen-

dence of the absolute mb intensity of $F_3P \cdot B_3H_5^+$ (*m/e* 126) is shown in Figure 12. The rapid decrease in intensity with increasing temperature and the relatively small intensity at 25° are consistent with pyrolysis of $F_3P \cdot B_3H_7$ at 25°. The complex was at least 95% decomposed at 90°. This decomposition behavior should have resulted in $F_3P \cdot B_3H_7$ acting as a good source of B_3H_7. The variation of mb intensity with increasing temperature for $B_3H_5^+$ (*m/e* 38), however, shows no increasing trend as observed with $(CH_3)_2NF_2P \cdot B_3H_7$ (Figure 4). Instead, both mb intensity and shutter effect (30–35%, *cf.* Figure 12) remain constant from 25 to 250°. All attempts to observe the formation of higher boranes, *e.g.*, B_5H_x, were unsuccessful.

Discussion

The synthesis of boron hydride reactive intermediates by thermal decomposition of their corresponding weak base–borane coordination compounds[8-10,14] has been extended successfully to triborane (7). It had been expected from a base-displacement reaction described by Paine and Parry[15] that $F_3P \cdot B_3H_7$ would be a better source of B_3H_7 than $(CH_3)_2NF_2P \cdot B_3H_7$. Our mb mass spectrometric investigations have shown that $F_3P \cdot B_3H_7$ was significantly decomposed in the reactor at low temperatures (25–90°), but B_3H_7 was not detected in the decomposition products from 25 to 250°. Instead a very intense $B_4H_x^+$ ion envelope was observed. An adequate rationalization of these results must await more detailed decomposition studies which would employ a cooled inlet system and reactor.

$$F_3P \cdot B_3H_7 + (CH_3)_2NF_2P \longrightarrow F_3P + (CH_3)_2NF_2P \cdot B_3H_7$$

A complex decomposition chemistry for $(CH_3)_2NF_2P \cdot B_3H_7$ was revealed by this mass spectrometric study. At 25° two species were observed in the vapors effusing from the reactor. The compounds were identified as the expected $(CH_3)_2NF_2P \cdot B_3H_7$ and an unexpected, but known, compound $(CH_3)_2NF_2P \cdot B_4H_8$.[33] This result and the important differences between the conventional and mb mass spectra of $(CH_3)_2NF_2P \cdot {}^nB_3H_7$ may be rationalized in light of the thermal decomposition studies. The observed smaller ion intensities for $L \cdot B_3H_x^+$ and the larger ion intensities for $B_6H_x^+$, $B_5H_x^+$, $B_4H_x^+$, and $B_3H_x^+$ in the conventional mass spectrum would be expected if pyrolysis of $(CH_3)_2NF_2P \cdot B_3H_7$ took place on the hot surfaces (125° or higher) of the conventional ion source. Our *controlled* mb decomposition studies verify the expectation. The mb study has conclusively shown that $(CH_3)_2NF_2P \cdot B_3H_7$ decomposed (ion intensity decreased) with increasing reactor temperature (Figure 2) and that the decomposition was *ca.* 40% complete at 125°. Furthermore, decomposition at this temperature was accompanied by the formation of $B_3H_x^+$, $B_4H_x^+$, $B_5H_x^+$, and $B_6H_x^+$ ions (Figures 4, 5, 8, 9). Similar observations were made in a recent mb mass spectrometric study of OCB_4H_8.[10]

The appearance of $(CH_3)_2NF_2P \cdot B_4H_8$ in the mb mass spectrum was unexpected since the purity of the $(CH_3)_2NF_2 \cdot B_3H_7$ samples had been independently verified by melting point determination and ^{19}F nmr spectroscopy. This finding requires that $(CH_3)_2NF_2P \cdot B_4H_8$ was formed in the inlet system of the spectrometer. Furthermore, inlet valve open–closed experiments suggest that the neutral compounds $L \cdot B_3H_7$ and $L \cdot B_4H_8$ undergo surface sorption at 25°. These facts argue for the formation of $L \cdot B_4H_8$ in the inlet system by a surface initiated decomposition of $L \cdot B_3H_7$.

The *thermal* decomposition of $(CH_3)_2NF_2P \cdot B_3H_7$ at 175° provided the first conclusive synthesis of the triborane(7) intermediate. The variation in ion intensity and shutter effect with temperature (Figure 4), shutter profiles, mass spectra (Figures 7, 10), ion intensity ratios (Figure 6), and appearance potentials (Table I) have provided an unambiguous characterization of B_3H_7. Similarly, the decomposition of $(CH_3)_2NF_2P \cdot B_4H_8$ has provided an additional characterization of B_4H_8. The formation of pentaborane(s) (Figure 8) and hexaborane(s) (Figure 9) with increasing reactor temperature has also been demonstrated. A comparison of respective shutter effects is noteworthy. The pentaborane ions, *e.g.*, $B_5H_7^+$ exhibited a relatively constant shutter effect from 25 to 250°, indicating that the neutral progenitor(s) was a stable borane. The hexaborane ions, *e.g.*, $B_6H_6^+$, however, showed a distinct increase in shutter effect (maximum at *ca.* 60% at 120°). The large shutter effect suggests that the neutral progenitor may have been a reactive borane, *e.g.*, B_6H_{14} or *i*-B_6H_{12} instead of a more stable borane, *e.g.*, B_6H_{10} or *n*-B_6H_{12}.[34]

The chemistry of $(CH_3)_2NF_2P \cdot B_3H_7$ in our inlet and reactor system may be summarized by the following net flow reaction

$$\begin{array}{l} [L \cdot B_3H_7 \sim\sim S] \xleftarrow{25^\circ} L \cdot B_3H_7 \xrightarrow{100\text{–}200^\circ} B_3H_7^* \\ \quad\downarrow \\ [L \cdot B_4H_8 \sim\sim S] \xrightarrow{25^\circ} L \cdot B_4H_8 \xrightarrow{125\text{–}250^\circ} B_4H_8^* \end{array} \Bigg] \longrightarrow \begin{array}{l} B_5H_x \\ + \\ B_6H_y^* \longrightarrow B_6H_y \end{array}$$

where $\sim\sim S$ and * imply surface coordination and reactive intermediate, respectively. The various details of the process await further study.

Some further conclusions may be drawn from the mass spectra of triborane(7) (Figures 7, 10; Table II). Several workers[3,35] have classified boron hydrides into relatively distinct groups. The groups with empirical formulas B_nH_{n+4} and B_nH_{n+6} have been referred to as "stable" and "unstable" boranes, respectively. It has been noticed that the "stable" boron hydrides display an intense parent ion peak, $B_nH_{n+4}^+$,[34,36] and fragment less than the unstable boranes. It has also been noticed that boron hydrides with terminal BH_2 group(s) are often chemically less stable and tend to fragment more (smaller parent ion) on electron impact than boranes without a BH_2 group. It is not coincidental then that "unstable" boranes (B_nH_{n+6}) generally contain a BH_2 group.

Prior to this study the only boron hydride known to violate the "stable" strong parent-ion intensity rule was B_2H_6.[34] The small parent-ion intensity for $B_3H_7^+$ ("stable"), however, represents an additional break-

(33) G. L. TerHaar, Ph.D. Thesis, University of Michigan, Ann Arbor, Michigan, 1961.

(34) S. J. Steck, G. A. Pressley, Jr., F. E. Stafford, J. Dobson, and R. Schaeffer, *Inorg. Chem.*, **9**, 2452 (1970), and summary references therein.

(35) R. W. Parry and L. J. Edwards, *J. Amer. Chem. Soc.*, **81**, 3554 (1959).

(36) J. F. Ditter, J. R. Spielman, and R. E. Williams, *Inorg. Chem.*, **5**, 118 (1966).

down of this qualitative rule. Its small intensity could be rationalized by the presence of one or more BH_2 groups in B_3H_7.[37]

(37) W. N. Lipscomb "Boron Hydrides," W. A. Benjamin, New York, N. Y., 1963, p 44. Two styx topological representations are predicted for B_3H_7, 3011 and 2102 containing one or two BH_2 groups, respectively.

Acknowledgments—The authors thank Professor Riley Schaeffer for a sample of $(CH_3)_4N \cdot B_3H_8$ and Professors Robert W. Parry and G. Kodama for a sample of $^nB_4H_{10}$ and the use of their laboratories for the synthesis of one of the $(CH_3)_2NF_2P \cdot {}^nB_3H_7$ samples.

CONTRIBUTION FROM THE SCHOOL OF CHEMICAL SCIENCES, UNIVERSITY OF ILLINOIS, URBANA, ILLINOIS 61801

X-Ray Photoelectron Spectra and Molecular Orbital Interpretation of the Valence Region of Cyanide and Nitrate

BY WILLIAM H. MORRISON, JR., AND DAVID N. HENDRICKSON*

Received March 29, 1972

X-Ray photoelectron spectra were determined for KNO_3 and NaCN in the valence region of 0–40 eV binding energy. In the case of KNO_3, four nonpotassium peaks (26.27, 14.59, 11.56, and 7.46 eV) and two potassium peaks (K_{3s}, 33.40 eV; K_{3p}, 17.37 eV) were detected. In the case of NaCN, five nonsodium peaks (24.67, 16.98, 12.76, 8.96, and 5.28 eV) and one sodium peak (Na_{2p}, 30.52 eV) were found. Extended Hückel, CNDO, and INDO molecular orbital calculations were carried out on nitrate and cyanide and an *ab initio* MO calculation was completed for cyanide. Peak assignments were advanced on the basis of these MO calculations.

Introduction

Inorganic applications of X-ray photoelectron spectroscopy (XPS)[1] have been mainly in the area of studying core-electron binding energies. Chemical shifts of core-electron binding energies have been noted for a large number of elements, and for many of these elements correlations have been established between the core-electron binding energies and atomic charges calculated by molecular orbital treatments (*e.g.*, nitrogen,[2,3] phosphorus,[4,5] boron,[6] and iron[7]). In some cases structural information has been inferred from these correlations.

Recently XPS has been used to study the valence region of various molecules in the gas phase.[8] The observed peaks in the XPS spectra of these gaseous samples have, in many cases, been assigned to the photoionization of electrons from filled molecular orbitals. Interesting comparisons have been made between XPS and ultraviolet photoelectron spectroscopy data for some molecules. Very recently Prins and Novakov[9] reported the XPS valence region (*i.e.*, 0–40 eV binding energy) spectra of *solid* samples of many different perchlorate and sulfate salts. They were able to assign the observed noncation peaks to the photoionizations of electrons from the filled molecular orbitals of the anions. In this paper we report the results of a similar study of salts of nitrate and cyanide.

(1) K. Siegbahn, C. Nordling, A. Fahlman, R. Nordberg, K. Hamrin, J. Hedman, G. Johansson, T. Bergmark, S.-E. Karlsson, J. Lindgren, and B. Lindgerg, "ESCA Atomic Molecular and Solid State Structure Studied by Means of Electron Spectroscopy," Almqvist and Wiksells AB, Stockholm, 1967.

(2) J. M. Hollander, D. N. Hendrickson, and W. L. Jolly, *J. Chem. Phys.*, **49**, 3315 (1968).

(3) D. N. Hendrickson, J. M. Hollander, and W. L. Jolly, *Inorg. Chem.*, **8**, 2642 (1969).

(4) M. Pelavin, D. N. Hendrickson, J. M. Hollander, and W. L. Jolly, *J. Phys. Chem.*, **74**, 1116 (1970).

(5) W. E. Morgan, W. J. Stec, R. G. Albridge, and J. R. Van Wazer, *Inorg. Chem.*, **10**, 926 (1971).

(6) D. N. Hendrickson, J. M. Hollander, and W. L. Jolly, *ibid.*, **9**, 612 (1970).

(7) L. N. Kramer and M. P. Klein, *Chem. Phys. Lett.*, **8**, 183 (1971).

(8) K. Sieghbahn, C. Nordling, G. Johansson, J. Hedman, P. F. Heden, K. Hamrin, U. Gelius, T. Bergmark, L. O. Werme, R. Manne, and Y. Baer, "ESCA Applied to Free Molecules," North-Holland Publishing Co. and American Elsevier, New York, N. Y., 1969.

(9) R. Prins and T. Novakov, *Chem. Phys. Lett.*, **9**, 593 (1971).

Experimental Section

Magnesium Kα X-radiation was used to excite the photoelectrons whose energies were analyzed using the Berkeley magnetic-focusing spectrometer. The powdered samples were deposited on double-faced adhesive tape; peak positions were measured *vs.* the C_{1s} signal (E_b = 285.0 eV) from the pump oil contaminant. The work function of the spectrometer was taken as 4.0 eV.

Calculations

CNDO(2) and INDO molecular orbital programs were taken from Pople and Beveridge's book.[10] The *ab initio* calculations were completed using QCPE104, "McLyosh Linear Molecule Program I," written by McLean and Yoshimine. Modified CNDO(1) calculations were completed as described previously.[11] In the extended Hückel calculations, coulomb integrals, H_{ii}, were approximated by valence-state ionization potentials.[12] The off-diagonal elements were assigned as

$$H_{ij} = 1.75S_{ij}(H_{ii} + H_{jj})/2$$

where S_{ij} is the overlap integral between the ith and jth atomic orbitals. Simple iterative extended Hückel molecular orbital calculations were carried out by performing a Mulliken population analysis on each cycle and correcting the valence-state ionization potentials for net atomic charge q_i

$$H_{ii} = H_{ii}^\circ - (2.0 \text{ eV/charge})q_i$$

The Slater atomic orbital exponents were taken as neutral atom orbital values, μ_i°, corrected for charge.

(10) J. A. Pople and D. L. Beveridge, "Approximate Molecular Orbital Theory," McGraw-Hill, New York, N. Y., 1970.

(11) P. M. Kuznesof and D. F. Shriver, *J. Amer. Chem. Soc.*, **90**, 1683 (1968).

(12) J. Hinze and H. H. Jaffe, *ibid.*, **84**, 540 (1962).